Oncology Research, Vol. 22, pp. 1–12
Printed in the USA.

0965-0407/14 $90.00 + .00
DOI: http://dx.doi.org/10.3727/096504014X14077751730270
E-ISSN 1555-3906
www.cognizantcommunication.com

ENOX2 Target for the Anticancer Isoflavone ME-143

D. James Morré, Theodore Korty, Christiaan Meadows, Laura M. C. Ades, and Dorothy M. Morré

Mor-NuCo, Inc., West Lafayette, IN, USA

ME-143 (NV-143), a synthetic isoflavone under clinical evaluation for efficacy in the management of ovarian and other forms of human cancer, blocked the activity of a cancer-specific and growth-related cell surface ECTO-NOX protein with both oxidative (hydroquinone) and protein disulfide-thiol interchange activity designated ENOX2 (tNOX) and inhibited the growth of cultured cancer cells with EC_{50}s in the range of 20–50 nM. Purified recombinant ENOX2 also bound ME-143 with a K_d of 43 (40–50) nM. Both the oxidative and protein disulfide-thiol interchange activities of ENOX proteins that alternate to generate a complex set of oscillations with a period length of 22 min compared to 24 min for the constitutive counterpart ENOX1 (CNOX) that characterizes ENOX proteins responded to ME-143. Oxidation of NADH or reduced coenzyme Q_{10} was rapidly blocked. In contrast, the protein disulfide-thiol interchange activity measured from the cleavage of dithiodipyridine (EC_{50} of ca. 50 nM) was inhibited progressively over an interval of 60 min that spanned three cycles of activity. Inhibition of the latter paralleled the inhibition of cell enlargement and the consequent inability of inhibited cells to initiate traverse of the cell cycle. Activities of constitutive ENOX1 (CNOX) forms of either cancer or noncancer cells were unaffected by ME-143 over the range of concentrations inhibiting ENOX2. Taken together, the findings show that ME-143 binds to ENOX2 with an affinity 4 to 10 times greater than that reported previously for the related anticancer isoflavone, phenoxodiol.

Key words: ENOX; NADH oxidase; ENOX2; Cancer; ME-143; NV-143; Phenoxodiol; Isoflavone; tNOX

INTRODUCTION

ME-143 (NV-143) [2H-1-benzopyran-7-0,1,3-(4-hydroxyphenyl)] (Fig. 1) is a synthetic anticancer isoflavone chemically related to natural isoflavone phytoestrogens such as genistein and the anticancer isoflavone-phenoxodiol (1–6). ME-143 is currently under clinical evaluation with refractory solid tumors and for its ability to synergize with platinum-base chemotherapy with focus on ovarian cancer. A phase I pharmacokinetic and safety study has been completed (7). Further trials are anticipated paralleling those previously conducted with phenoxodiol (8–10).

The present study is to validate a cancer-specific cell surface protein, ENOX2, previously identified as the molecular target of phenoxodiol (6) as the molecular target of ME-143 through direct binding to recombinant ENOX2 and through the inhibition of the protein disulfide-thiol interchange and oxidative activities of ENOX2. ENOX2 is a form of growth-related cell surface oxidase (ECTO-NOX) specific to cancer cells. The protein disulfide-thiol interchange activity catalyzed by ENOX2 correlates with the enlargement phase of cell growth (11,12).

The study is based on the discovery in our laboratories of a cancer-specific and growth-related cell surface hydroquinone oxidase with protein disulfide-thiol interchange activity, referred to as ENOX2 (13), as the potential molecular target for ME-143 to help explain both it selectivity for cancer cells and its apparent pan-cancer pattern of efficacy (7). ENOX2 is associated with a wide variety of human cancers, including leukemias, lymphomas, carcinomas, and sarcomas (14,15). ENOX2 was originally recognized as distinct from other cell surface and internal oxidases on the basis that its activity was blocked by several quinone site inhibitors, all with anticancer activity (16–20). In addition to phenoxodiol (6), ENOX2 has been independently confirmed as a cell surface target for antitumor sulfonylureas (14), the vanilloid capsaicin (18), and the anticancer green tea catechins (18,19).

MATERIALS AND METHODS

Materials

ME-143 and phenoxodiol were from Marshall Edwards, Inc. (11975 El Camino Real, Suite 101, San Diego, CA, USA). All other chemicals were from Sigma (St. Louis, MO, USA) or from suppliers indicated.

Expression of Recombinant ENOX2

Recombinant ENOX2 was expressed by *E. coli* [BL21 (DE3)]. Proteins were extracted from *E. coli* by using a motor-driven laboratory press equipped with a standard

Address correspondence to D. James Morré, Mor-NuCo, Inc., 1201 Cumberland Avenue, Suite B, Purdue Research Park, West Lafayette, IN 47906, USA. Tel: +1-765-491-4876; Fax: +1-765-464-8769; E-mail: dj_morre@yahoo.com

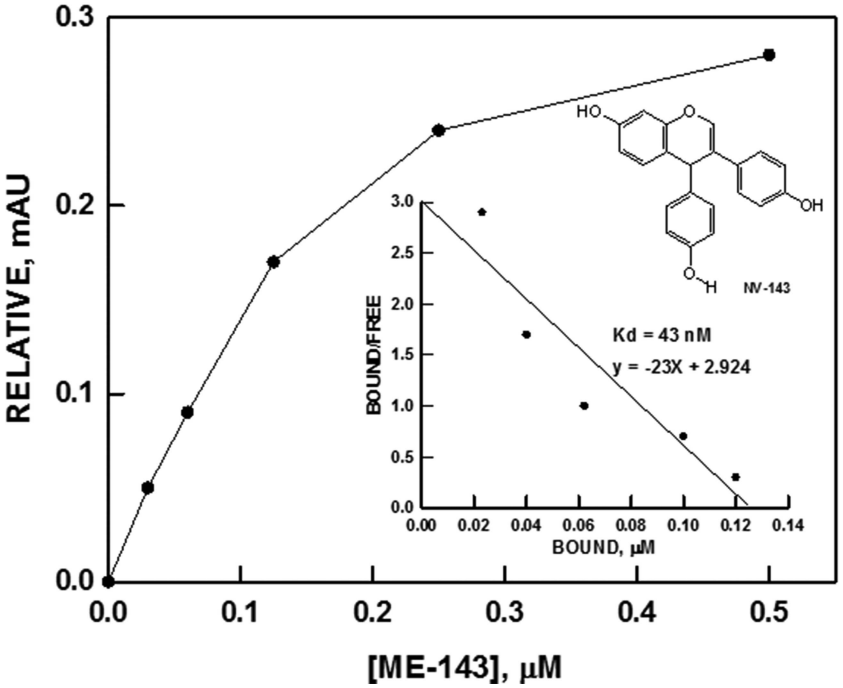

Figure 1. Binding of ME-143 to purified recombinant ENOX2 (135 g) determined by equilibrium dialysis (20) over the range 0–0.5 M. The inset shows the Schatchard analysis of binding. Results indicated a high-affinity binding component with a K_d of about 43 (40–50) nM.

French pressure cell (Thermo Electron Corporation, Needham Heights, MA, USA). Recombinant ENOX2 was purified by ammonium sulfate precipitation (60%), anion-exchange chromatography, and gel-filtration chromatography. The purified protein was >90% pure as determined from the intensity of silver-stained SDS-polyacrylamide gels.

Equilibrium Binding

For binding studies, a multicell rotating Teflon cell equilibrium dialyzer (Spectrum Equilibrium Dialyzer, Spectrum Medical Instruments, Los Angeles, CA, USA) with a dialyzing volume of 1 ml and a 47-mm diameter membrane 12 to 14 kDa molecular mass exclusion was used (20).

The dialysis membranes were prepared by soaking in distilled water for 30 min followed by 30% ethanol for 30 min and several changes of distilled water at room temperature. Both sides of the chamber were supplied with 1 ml final volume of 50 mM Tris HCl (pH 7.5). To one side of each chamber were added the ME-143 in DMSO and recombinant ENOX2 (7 g of soluble ENOX2 monomer). An equivalent amount of DMSO was added to the opposite side of the chamber and equilibrium established by rotating the cells at about 100 rpm at 24°C overnight. A 1-ml sample was withdrawn from each chamber, and ME-143 was determined by HPLC analysis. Determinations were in triplicate (Fig. 1) to increase the confidence of specific high-affinity binding to approximately ±5%.

Growth of Cells

Cells were grown in culture in a humidified atmosphere of 5% CO_2 in air at 37°C. Media were renewed every 2 to 3 days.

HeLa (ATCC CCL-2) human cervical adenocarcinoma cells were cultured in minimal essential medium (Eagle's) with 1 mM L-glutamine and Earle's balanced salt solution adjusted to contain 1.5 g/L sodium bicarbonate, 0.2 mM nonessential amino acids, 1.0 mM sodium pyruvate, and supplemented with 10% fetal bovine serum (heat inactivated) plus 50 mg/L gentamicin sulfate.

MCF-10A (ATCC CRL-10317) human mammary noncancer epithelial cells were cultured in a 1:1 mixture of Ham's F12 medium and Dulbecco's modified Eagle's medium containing insulin (10 mg/L), hydrocortisone (0.5 mg/L), epidermal growth factor (20 mg/L), and supplemented with 5% horse serum (heat inactivated) plus 50 mg/L gentamicin sulfate.

BT-20 (ATCC HTB19) human mammary adenocarcinoma cells were cultured in Eagle's minimal essential medium containing 0.1 mM nonessential amino acids, 1.0 mM sodium pyruvate, and 50 mg/L gentamicin sulfate supplemented with 10% fetal bovine serum (heat inactivated).

Spectrophotometric Assay of Enzymatic Activities

Oxidation of NADH was determined from the disappearance of NADH measured at 340 nm (21) in a reaction mixture containing 25 mM Tris-MES (pH 7.2),

100 M GSH, 1 mM KCN to inhibit mitochondrial oxidase activity, and 150 μM NADH at 37°C with temperature control (±0.5°C) and stirring (22). Activities were measured using paired Hitachi U3210 spectrophotometers with continuous recording. Assays were initiated by the addition of NADH. Assays were for 1 min and were repeated on the same sample every 1.5 min for the times indicated. An extinction coefficient of 6.22 cm^{-1} mM^{-1} was used to determine specific activity.

Protein disulfide-thiol interchange was determined from the cleavage of an artificial dithiodipyridine substrate (23). Hydroquinone oxidase activity was estimated as previously described (24) from absorbance changes at 275 and 410 nm (25,26) with reduced coenzyme Q_{10} (Tishcon, Westbury, NY, USA) as the substrate.

Proteins were estimated by the bicinchoninic acid method (27). Bovine serum albumin was the standard.

Antisense Oligonucleotide Synthesis

Oligonucleotide E5AS and its corresponding scrambled control E5C were synthesized and desalted by Integrated DNA Technologies (IDT, Inc., Coralville, IA, USA). There were three phosphorothioated linkages at each end of the oligonucleotides. The sequences are E5AS 5 -GTC TGCCTGTGTCCTTCTTGT-3 (nucleotide 600 to 620 of tNOX) and E5C 5 -CCCGGCTTGGTTTTGCTTTTC-3 .

Transfection of Cultured HeLa Cells With Antisense Oligonucleotides

One day before in vitro transfection, HeLa cells were plated in 10-cm tissue culture plates. Antisense oligonucleotides were delivered into cells with Lipofectamine 2000 (Invitrogen, Grand Island, NY, USA).

Cytotoxicity Assays

Cells were subcultured into 96-well culture plates at 2×10^4 densities and permitted to adhere for 8–12 h at 37°C. The cells were washed once with sterile phosphate-buffered saline, pH 7.2, and treated with increasing concentrations of phenoxodiol or ME-143 (prepared in ethanol) or ENOX2 polyclonal antisera (preimmune sera were used as control). Cell viability was assessed using the MTT assay. Cell viability was expressed as the percentage of viable cells relative to untreated cells using the absorbance at 450 nm. All experiments were performed in triplicate in at least three separate experiments.

Growth Measurements

Cell growth was determined using a 96-well plate assay. Cells were fixed by glutaraldehyde and stained with 1% aqueous crystal violet. Absorbance was determined at 580 nm with an automated plate reader. Cell number was determined microscopically by counting the number of cells over defined areas consisting of a grid of 1-mm squares.

Statistical Analyses

Results were analyzed using fast Fourier transform and decomposition fits (28). To determine the period length of activity oscillations, the fast Fourier transforms were with a user-defined transform in Sigma Plot 8.0. Decomposition fits on both the enzyme activity and the growth determinations used MINITAB and were based on the period length established by Fourier analysis.

RESULTS

ME-143 Binding to Recombinant ENOX2

The purified recombinant ENOX2-bound ME-143 was determined by equilibrium dialysis (Fig. 1). The K_d for high-affinity binding was 43 (40–50) nM. The relative number of high-affinity sites was similar to that for phenoxodiol and approximately equal to 1 nmol/nmol of soluble recombinant ENOX2 monomer.

Antiproliferative Effects of ME-143 in Human Cancer Cell Lines

Exponentially growing cell lines were exposed to increasing concentrations of either ME-143 or phenoxodiol (Table 1). A significant decrease in cell number was observed, which correlated with inhibition of NADH oxidation reaching IC_{50} concentrations at 48 h for HeLa (human cervical carcinoma) of 50 nM for ME-143 and 200 nM for phenoxodiol and at 20 nM for ME-143 and at 6 M for phenoxodiol with BT-20 (human mammary adenocarcinoma) cell lines, respectively (Table 1). The ultimate result was a population of small cells unable to divide further, which subsequently underwent apoptosis. For noncancer MCF-10A (human mammary epithelia), the IC_{50} exceeded 0.5 M for ME-143 and 20 M for phenoxodiol. With three human ovarian carcinoma cell lines, A2780, R-182, and CP70, the IC_{50}s (μM) for ME-143 were 0.47, 0.13, and 0.51, respectively (unpublished preclinical results, Marshall Edwards, San Diego, CA with permission). For a cancer cell line with significantly reduced ENOX2, HeLa cells were transfected with exon 5 ENOX2 antisense that recognizes exon 4 minus messenger RNA. Under conditions where a reduction of exon 4 minus mRNA of ca. 80% was achieved (29), the IC_{50} for ME-143 was greater than 300 nM.

Table 1. Dose Response of HeLa (Human Cervical Adenocarcinoma) or BT-20 (Human Mammary Adenocarcinoma) Cells Comparing Phenoxodiol and ME-143 and Response of MCF-10A (Human Mammary Noncancer) Cells

	IC_{50} 48 h (μM)	
Cell line	Phenoxodiol	ME-143
HeLa	0.2 ± 0.025	0.05 ± 0.02
BT-20	6.0 ± 4.0	0.02 ± 0.007
MCF-10A	>20	>0.5

NADH Oxidation by ENOX2 Is Inhibited by ME-143

NADH oxidation by recombinant ENOX2 was inhibited in parallel to direct binding based on disappearance of NADH measured at A_{340} (Fig. 2A) with an EC_{50} of about 50 nM (Fig. 3). Inhibition was observed on the HeLa cell surface both with native ENOX2 (Fig. 4A) and with ENOX2 released from the surface of the HeLa cells (Fig. 4B) by treatment with 0.1 M sodium acetate, pH 5 for 2 h at 37°C (30). Inhibitory concentrations of ME-143 were without effect on the NADH oxidase activity of

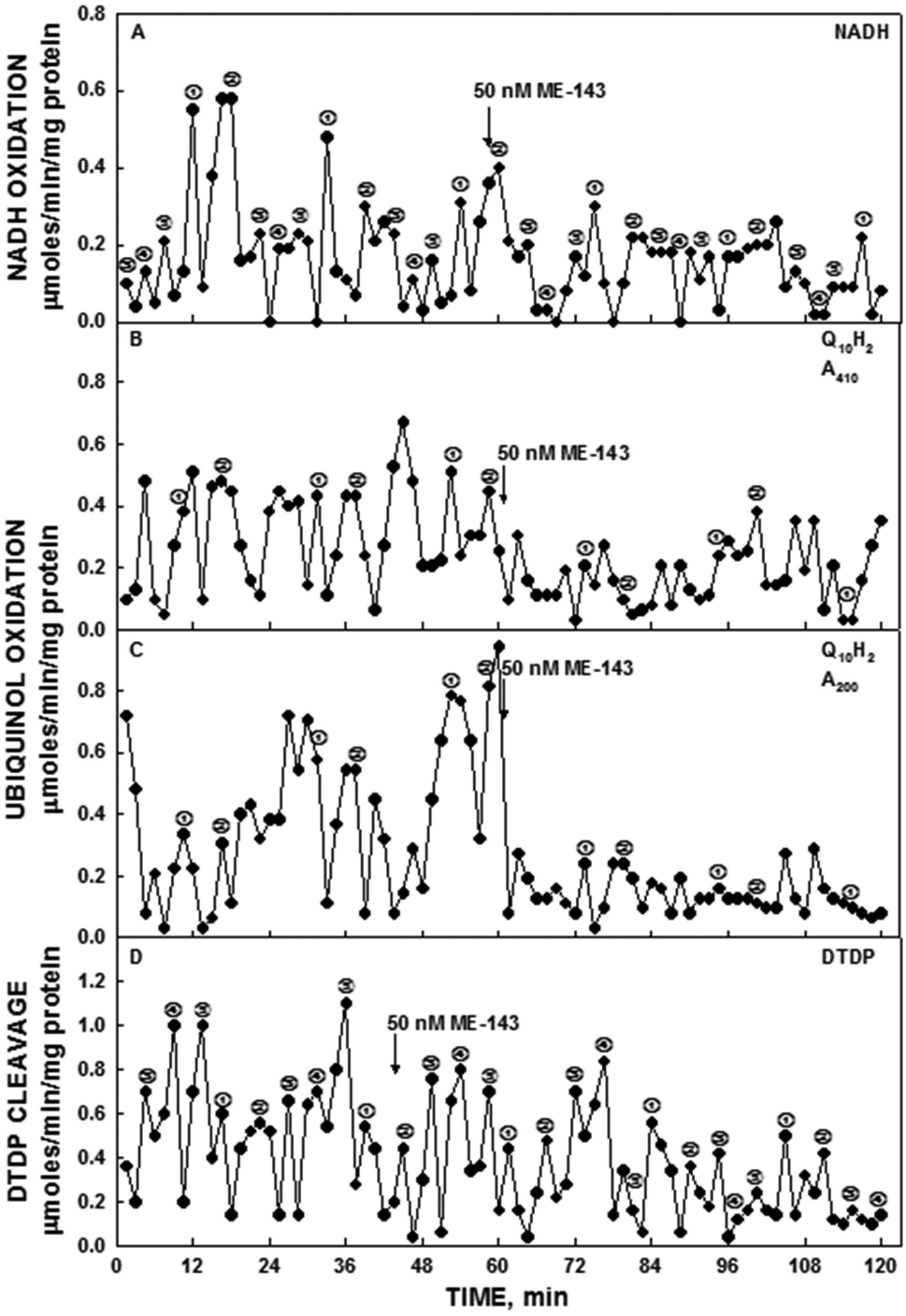

Figure 2. Activity of recombinant ENOX2. Comparison of the response of recombinant ENOX2 to addition of 50 nM ME-143 added after 48 min (arrow) comparing each of the four available assays on aliquots of the same ENOX2 preparations. NADH (A) or hydroquinone oxidation (B, C). Protein disulfide-thiol interchange measured by DTDP cleavage (D) was inhibited after about 60 min. (B) and (C) were determined simultaneously at the two different wavelengths and were directly comparable.

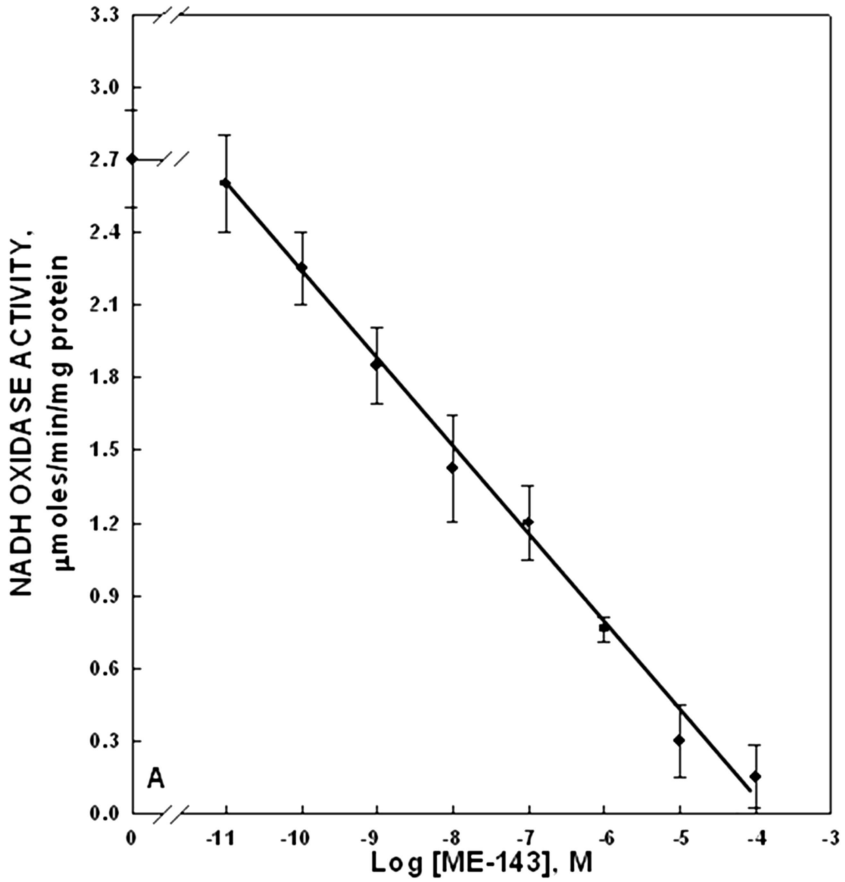

Figure 3. Dose response of NADH oxidase activity of recombinant ENOX2 as a function of the log ME-143 concentration. The EC_{50} was approximately 50 nM. Average of two determinations ± mean average deviations.

noncancer MCF-10A mammary epithelia, which lack ENOX2 activity, and on the ENOX1 activities of HeLa cells (Fig. 4). The IC_{50} of inhibition of recombinant ENOX2 and of the ENOX2 of HeLa cells of about 50 nM correlated with the EC_{50} of binding to recombinant ENOX2 (Fig. 1) and for inhibition of growth of HeLa cells (Table 1).

ME-143 Prevents ENOX2 From Oxidizing Reduced Plasma Membrane Quinones, the Physiological Substrate, for the Oxidative Portion of the ECTO-NOX Cycle

Oxidation of reduced plasma membrane quinones such as ubiquinol is considered to be the principal physiological function of the oxidative portion of the ECTO-NOX cycle (24). Hydroquinone oxidation by ENOX2 was blocked almost immediately by ME-143 as measured either from the increase in absorption at 410 nm (Fig. 2B) or the decrease in absorption at 290 nm (Fig. 2C). Measurements at both wavelengths are taken to ensure specificity of the assay for coenzyme Q oxidation.

Inhibition of ENOX2-Catalyzed Protein Disulfide-Thiol Interchange by ME-143

The protein disulfide-thiol interchange activity of HeLa cells as measured from the cleavage of an artificial protein disulfide-thiol interchange substrate, dithiodipyridine (DTDP), was inhibited as well by ME-143 (Fig. 2D). Inhibition by ME-143 was progressive and complete only after about 60 min of ME-143 treatment.

By the method used, the activity during the protein disulfide-thiol interchange portion of the cycle was revealed as three distinct maxima. The three maxima, numbered ③, ④, and ⑤, were separated by intervals of 4 min and recurred at intervals of 22 min compared to a 4.5-min separation and recurrence at 24 min for the protein disulfide-thiol interchange activity of the constitutive ENOX1. The sequential nature of the inhibition of protein disulfide-thiol interchange by ME-143 was apparent within the repeating pattern of the three maxima. In the second full cycle following ME-143 addition, the maximum marked ⑤ was lost. In the third full cycle following

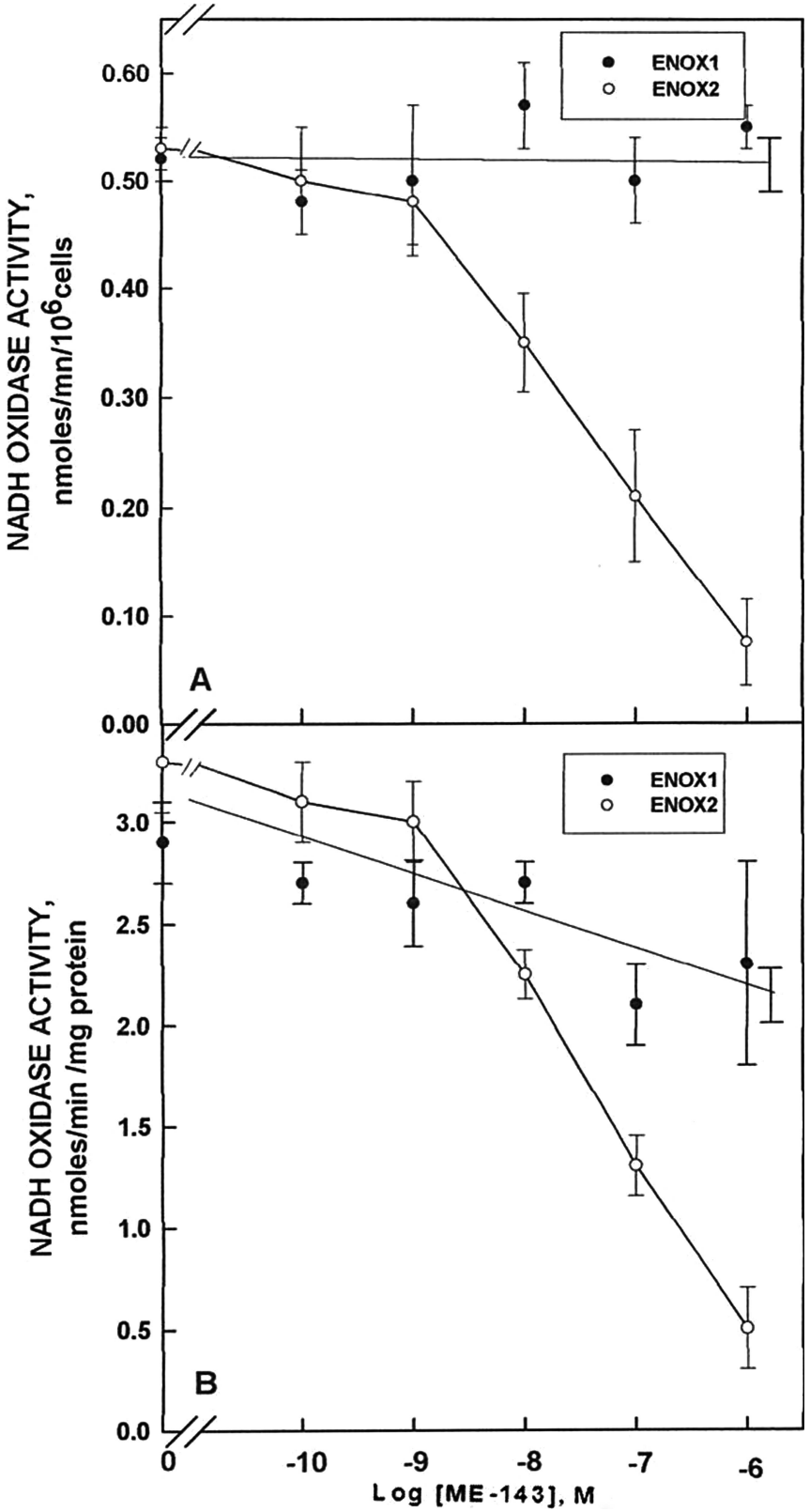

Figure 4. Dose response of NADH oxidase activity comparing ENOX1 (solid symbols) and ENOX2 (open symbols) of intact HeLa cells (A) and a soluble ENOX preparation are released from the HeLa cell surface by treatment with 1 M sodium acetate, pH 4.0 for 2 h at 37°C (30) (B). The EC_{50} for inhibition was about 50 nM for both sources of ENOX2, whereas ENOX1 activity was unaffected (A) or was much less responsive (B). Average of 3 to 5 determinations ± standard deviations.

Table 2. Progressive Loss of Maxima ③, ④, and ⑤ of the ENOX Activity Cycle of Recombinant ENOX2 Upon Treatment With 50 nM ME-143 Based on Analyses of DTDP Cleavage Assays (Average of Five Experiments ± Standard Deviations)

	Control (μmol/min/mg/protein)			10 μM ME-143 (μmol/min/mg/protein)		
	③	④	⑤	③	④	⑤
Period 1	0.92 ± 0.30	0.92 ± 0.18	0.92 ± 0.24	0.80 ± 0.34	0.62 ± 0.20	0.84 ± 0.20
Period 2	0.80 ± 0.14	0.90 ± 0.24	0.80 ± 0.22	0.66 ± 0.12	0.70 ± 0.08	0.34 ± 0.08
Period 3	0.76 ± 0.06	0.76 ± 0.06	0.76 ± 0.06	0.48 ± 0.10	0.34 ± 0.10	0.30 ± 0.10
Period 4	0.76 ± 0.12	0.70 ± 0.06	0.72 ± 0.06	0.24 ± 0.12	0.17 ± 0.03	0.28 ± 0.06

ME-143 addition, the maximum marked ④ was lost, and in the fourth full cycle following ME-143 addition, all three maxima ③, ④, and ⑤ were reduced to baseline. These data were quantitated as shown in Table 2.

ME-143 Effects on Protein Disulfide-Thiol Interchange Activities Are Cancer Cell Specific and Dose Dependent

With MCF-10A human mammary epithelial (noncancer) cells and plants (soybean), both of which lack the putative ENOX2 ME-143 target, the cell surface protein disulfide-thiol interchange activities were unaffected by phenoxodiol at concentrations inhibitory to BT-20 mammary adenocarcinoma and HeLa cells. Similarly, elongation of soybean stem sections (not shown) and growth of MCF-10A cells (Table 1) also were largely unaffected by ME-143 at concentrations inhibitory to cancer cells. The EC_{50} of ME-143 for both inhibition of the protein disulfide-thiol interchange activity of ENOX2 and for inhibition of short-term growth of HeLa cells was estimated to be about 50 nM (Fig. 5).

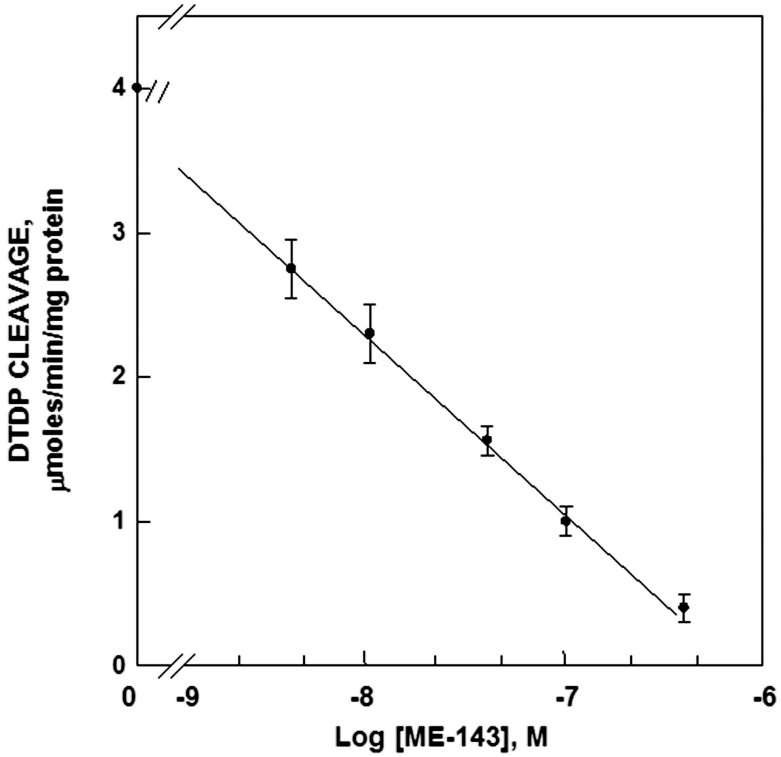

Figure 5. Dose response of protein disulfide-thiol interchange activity of recombinant ENOX2 as measured by DTDP cleavage (23). The EC_{50} was approximately 50 nM. Average of 2 determinations ± mean average deviations.

Table 3. Parameters of Phenoxodiol Inhibition of ENOX2 Activity ± Standard Deviations (N = 3) and Binding Determined in Parallel With That of ME-143

Parameter	EC_{50} (nM) ± SD
Phenoxodiol inhibition of activity of	
Recombinant ENOX2	330 ± 153
ENOX2 of the HeLa cell surface	340 ± 135
ENOX2 released from HeLa cell surface	320 ± 120
	kDa ± SD
Phenoxodiol binding to recombinant ENOX2	310 ± 96

Relative Efficacy of Binding of ME-143 Compared to Phenoxodiol

To determine the relative efficacy of binding of ME-143 and phenoxodiol, efficacy values for phenoxodiol were determined in parallel to those for MET-143 for comparison (Table 3). The response of NADH oxidase activity of ENOX2 of the HeLa cell surface (NADH is an impermeant substrate) and of ENOX2 stripped from the surface of HeLa cells and partially purified show EC_{50} values of between 200 and 500 nM (average 335 ± 144 nM) of phenoxodiol compared to 50 nM for ME-143. Also inhibited by phenoxodiol was the NADH oxidase activity of recombinant ENOX2 (average EC_{50} of 320 ± 120 nM).

Binding of phenoxodiol to recombinant ENOX2 reported previously revealed a high-affinity site of 50 nM (6), similar to that observed for ME-143 (Fig. 6). However, a second series of high-affinity sites of phenoxodiol binding, not observed with ME-143, also were evident from the data (6). Reevaluation of phenoxodiol binding over the range of 0.4 to 1.6 μM confirmed these findings with a kDa of 300 nM corresponding closely to the EC_{50} for inhibition of ENOX2 activity of HeLa cells and the activity of recombinant ENOX2 (Table 3).

DISCUSSION

ENOX2 is a cancer-specific form of a family of growth-related and time-keeping proteins of the cell surface (11) with both hydroquinone or NADH oxidation and protein disulfide-thiol interchange activities (ECTO-NOX proteins) (31) that responds to several known or putative quinone site inhibitors, all of which have anticancer activity (12). (−)-Epigallocatechin-3-gallate (19), capsaicin (18), adriamycin (32), and the antitumor sulfonylureas (14,33,34) were previously shown to inhibit both the NADH oxidation and protein disulfide-thiol interchange activities of ENOX2 with no effect on either activity of ENOX1 or growth of noncancer cells (16,31) as the basis for their cancer specificity. The synthetic isoflavone ME-143 inhibits both NADH and hydroquinone oxidation, as well as the protein disulfide-thiol interchange (6). NADH and hydroquinone oxidation are inhibited without a perceptible lag. Inhibition of the protein disulfide-thiol interchange portion

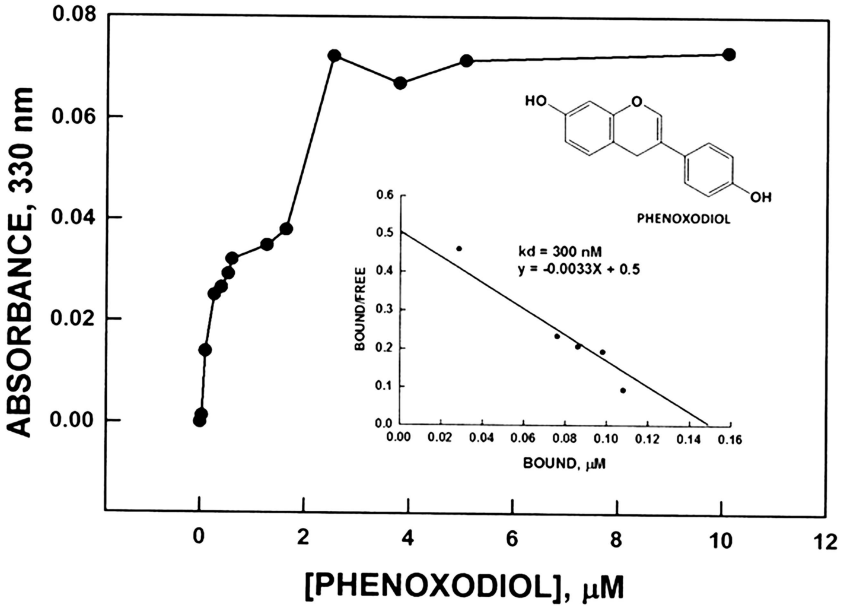

Figure 6. Binding of phenoxodiol to purified recombinant ENOX2 (135 μg) as determined by equilibrium dialysis over the range 0 to 12 μM. The inset shows a Schatchard analysis of binding over the range 0.4 to 1.6 μM phenoxodiol. Results indicate a binding component with a kDa of about 300 nM.

of the cycle, on the other hand, occurs sequentially as does the inhibition of cell enlargement by phenoxodiol (6) such that a complete cessation of growth is the eventual result of ME-143 addition followed 3 to 6 h later by apoptosis (3). The findings suggest that the isoflavone interacts differently with the conformational state of ENOX2 that carries out protein disulfide-thiol interchange, the portion of the NOX cycle that drives cell enlargement, than it does with the conformation state of ENOX2 that carries out the oxidative portion of the cycle.

NADH oxidation and hydroquinone oxidation were modulated differentially in a manner distinct from protein disulfide-thiol exchange also by the isoflavone phenoxodiol (6). The conserved NADH (adenine nucleotide-binding) motif of ENOX2 (confirmed by site-directed mutagenesis) is located beginning at T589 (full length) and is very near the carboxy-terminus of the protein (13). The conserved quinone binding site, which is also the drug binding site confirmed by site-directed mutagenesis, is located near the amino-terminus of fully processed ENOX2 beginning at E394 (full length) (13). In contrast, protein disulfide-thiol interchange is blocked by cysteine 505 and cysteine 569 replacements (13). The NADH site is located at the external cell surface and accessible to external NADH (33). The quinone site is presumably located nearer the plasma membrane surface and accessible to membrane-located hydroquinone. Occupancy of the quinone site by ME-143 would be expected to block hydroquinone oxidation as observed. The hydroquinone oxidation occurs without perceptible lag. Inhibition of protein disulfide-thiol interchange occurs more slowly and may relate to a more complicated insertion of phenoxodiol or ME-143 into the quinone site, resulting also in the inhibition of cell enlargement.

The pattern of progressive inhibitions by ME-143 of the enlargement phase of HeLa cells was similar to that previously observed with phenoxodiol, both for inhibition of protein disulfide-thiol interchange and for cell proliferation as determined from the increase in cell area quantitated by image-enhanced light microscopy (6). Inhibition of the latter was similar to the progressive pattern of inhibition of protein disulfide-thiol interchange activity of ENOX2 (Table 2). Cell enlargement also is cyclic (34) and occurs via a complex series of pulses (35). The phenoxodiol or ME-143-treated cells, unable to enlarge, are apparently unable to pass the G_1 checkpoint that monitors cell size (36) and, as a result, fail to proliferate and undergo apoptosis (3).

As has been shown to be a unifying characteristic of ECTO-NOX proteins, the two enzymatic activities they catalyze, NADH oxidation and protein disulfide-thiol interchange, alternate to generate a series of oscillations with a period length of 21 or 22 min (tumor-associated ENOX2) or 24 min (constitutive ENOX1). This alternation of activities is not a simple sine function but a repeating 2 + 3 pattern of maxima with maxima ① and ② favoring NADH (Fig. 2A) or hydroquinone (Fig. 2B, C) oxidation and maxima ③, ④, and ⑤ favoring protein disulfide-thiol interchange (Fig. 2D) and correlating with cell enlargement (11). In noncancer cells, the pattern repeats with a period length of 24 min suggestive of a clock or time-keeping function (37). The period length is independent of temperature and entrainable (38,39), both characteristics of the biological clock (40,41). Autoentrainment in solution results in the highly synchronous ECTO-NOX function observed experimentally. COS cells transfected with ECTO-NOX proteins having period lengths less than (22 min) or greater than (36 or 42 min) 24 min give rise to circadian period lengths in activity of glyceraldehyde-3-phosphate dehydrogenase of less than (22 h) or greater than (36 or 42 h) 24 h (37). In the transfected COS cells, the circadian day appears to be equal to 60 times the ECTO-NOX period.

The cancer-specific ENOX2 protein differs from the constitutive ECTO-NOX, ENOX1, primarily in being drug responsive (an EEMTE quinone/drug binding motif) (13) and having a shorter, 21 or 22 min, period length (35). The recombinant ENOX2 investigated, which carried a nus tag, exhibited a 21-min period length. Cancer cells and tissues express both ENOX1 and ENOX2. The cell surface expression of ENOX2 is the result of expression of a specific ENOX2 splice variant lacking exon 4.

Both ME-143 and phenoxodiol are potent inducers of apoptosis (1,3). Kamsteeg et al. (3) have characterized the apoptotic effect of phenoxodiol on ovarian cancer cells and provide evidence that the apoptotic effect is due to the regulation of the Akt–FLIP–XIAP pathway. Furthermore, they have demonstrated that the successful inactivation of FLIP and XIAP by phenoxodiol restores the sensitivity of ovarian cancer cells to Fas-mediated apoptosis through the Akt signal transduction pathway. Akt translocates to the nucleus where it may contribute to the regulation of the transcription of genes mediating cell survival. A possible mechanism by which Akt functions as a promoter of survival is through the induction of FLIP expression and blocking the extrinsic apoptotic pathway (42,43). Also, in this study, high levels of FLIP were found in all the ovarian cancer cells. When the effect of phenoxodiol on Akt was evaluated, a clear inhibition of its expression was followed by a decrease in FLIP expression and reversal of the sensitivity to Fas-mediated apoptosis.

In the studies of Kamsteeg et al. (3), phenoxodiol treatment resulted in a significant decrease in viability of ovarian cancer cells (IC_{50} of 1.35 M for CP70 cells) but was without effect on ovarian surface epithelial cells. Ovarian cancer cells in culture (OVCAR) do express ENOX2 (13). In clinical studies, phenoxodiol has proven to be nontoxic to normal human cells and tissues. The

interesting possibility that the extraordinary high level of safety and potential pan-cancer anticancer drug action of phenoxodiol might be related to the pan-cancer distribution of the ENOX2 target (14,15) and the absence of ENOX2 from noncancer cells and tissues, an argument that will extend as well to ME-143.

Direct links between inhibition of ENOX2 and induction of apoptosis were indicated early (1,3) and have only developed subsequently (44,45). Two consequences of inhibition of ENOX2 in cancer cells would be an accumulation of hydroquinone in the plasma membrane and decreased levels of cytosolic NAD^+ through conversion to NADH as a result of continued glycolytic activity in the absence of plasma membrane electron transport. Release of NAD^+ inhibition of sphingomyelinase through conversion to NADH would help account for a rise in ceramide and subsequent G_1 arrest resulting from phenoxodiol addition. Also provided is a possible link between pyridine nucleotide or hydroquinone levels and regulation of sphingosine kinase activity leading to activation of the FAS pathway of apoptosis.

ME-143 does reduce the ability of adherent cells to survive. However, our studies on apoptosis have thus far been restricted to late events, that is, using the BODIPY-duTP/TdT assay in HeLa cells beginning about 6 h posttreatment of fully attached cells.

A progressive, stepwise inhibition of an enzymatic activity by both phenoxodiol and ME-143 as was observed with the protein disulfide-thiol interchange activity appears to be unprecedented in the literature. EGCG and capsaicin, or other vanilloids, however, that inhibit in different parts of the NOX cycle exhibit strong synergies (46). It is as though access into the drug binding site is restricted to certain phases within the NOX cycle and that the site is inaccessible at other times. An extension of this concept would be that the fit of the ENOX2 drug site with phenoxodiol is such that entry into the drug site sufficient to inhibit completely the protein-disulfide interchange or ME-143 would require three full 22-min NOX cycles with the interchange activity attributable to each of the three maxima of the 2 + 3 pattern being inhibited sequentially as the drug enters the site.

In previous work, antisense experiments demonstrated an exon 4 minus splice variant mRNA as the basis for expression of the ME-143 target protein ENOX2 (29). Antisense to exon 5 mRNA inhibited both the production of exon 4 minus mRNA and the amount of ENOX2 associated with the cancer cell surface. Scrambled antisense for exon 5 minus mRNA was without effect. Compared to nontransfected HeLa cells, growth of HeLa cells transfected with exon 5 antisense growth inhibition was followed by apoptosis in greater than 70% of the cells. That the biological effects and cytotoxicity resulting from ENOX2-specific antisense were similar to those observed with ME-143 provide independent confirmation of ENOX2 as the potential ME-143 target protein.

The basis for growth inhibition and induction of apoptosis by all ENOX2 inhibitors thus far examined (16,19, 45,47,48) is that the drugs prevent cells once having divided to enlarge sufficiently to reach the minimum size to divide again. The resultant small cells, unable to enlarge and unable to divide, eventually undergo apoptosis.

The antiproliferative effects of phenoxodiol were more specifically shown by Aguero et al. (1) in head and neck squamous carcinoma cells to result from G_1 arrest. Failure to progress beyond G_1/S was the result of a specific loss in cyclin-dependent kinase 2 activity and p53-independent induction of $p21^{WAF1/CIP1}$ (1). As in our findings, the cell cycle arrest preceded apoptosis by several hours (12 h).

The unique inhibitory pattern for phenoxodiol and the related ME-143 may help explain their high degree of cancer specificity and the low toxicity to noncancer cells and tissues. Constitutive ECTO-NOX proteins, also responsible for enlargement of noncancer cells, are likely unable to bind either phenoxodiol or ME-143 and thus are protected from the cancer-specific drug toxicity. The pan-cancer nature of ENOX2 (all forms of human cancer) (12,13) may explain, as well, the broad-spectrum effectiveness of phenoxodiol against a wide range of human cancers including ovarian, breast, prostate, and leukemias (2–7). The ENOX2 target additionally offers a unique opportunity to understand how progressive binding of ME-143 with the drug-binding site of ENOX2 leads to inhibition of cell enlargement and subsequently to G_1 arrest and apoptosis either as a chemosensitizer (48–50) or as a single agent.

A direct comparison of ME-143 and phenoxodiol revealed a disparity in terms of effectiveness with ME-143 being 4 to 10 times more efficacious than phenoxodiol both in terms of inhibition of ENOX2 activity (Table 3) and in the inhibition of growth of cultured tumor cells (Table 1). Inhibition of recombinant ENOX2 by phenoxodiol with an EC_{50} of 330 ± 153 nM was comparable to the earlier determined EC_{50} of 200 nM (6). Based on binding data (Fig. 6, Table 3), it would appear that the greater efficacy of ME-143 may be due to a dependence more on the high-affinity sites at 50 nM compared to phenoxodiol that appears to depend more on high-affinity sites between 200 and 350 nM for inhibition of ENOX2 activity.

ACKNOWLEDGMENTS: We thank Debby Parisi for assistance with cell culture and for spectrophotometric measurements of enzymatic activities, and Peggy Runck for assistance with manuscript preparation.

REFERENCES

1. Aguero, M. F.; Facchinetti, M. M.; Sheleg, Z.; Senderowica, A. M. Phenoxodiol, a novel isoflavone, induces G1 arrest by specific loss in cyclin-dependent kinase 2 activity by p53-independent induction of p21WAF1/CIP1. Cancer Res. 65:3364–3373; 2005.

2. Brown, D. M.; Kelly, G. E.; Husband, A. J. Flavanoid compounds in maintenance of prostate health and prevention and treatment of cancer. Mol. Biotechnol. 30:253–270; 2005.
3. Kamsteeg, M.; Rutherford, T.; Sapi, E.; Hanczaruk, B.; Shahabi, S.; Flick, M.; Brown, D.; Mor, G. Phenoxodiol – an isoflavone analog – induces apoptosis in chemoresistant ovarian cancer cells. Oncogene 22:2611–2620; 2003.
4. Constantinou, A. I.; Husband, A. Phenoxodiol (2H-1-benzopyran-7-0,1,3-(4-hydroxyphenyl)), a novel isoflavone derivative, inhibits DNA topoisomerase II by stabilizing the cleavable complex. Anticancer Res. 22:2581–2585; 2002.
5. Constantinou, A. I.; Mehta, R.; Husband, A. Phenoxodiol, a novel isoflavone derivative, inhibits dimethylbenz[1] anthracene (DMBA)-induced mammary carcinogenesis in female Sprague-Dawley rats. Eur. J. Cancer 39:1012–1018; 2003.
6. Morré, D. J.; Chueh, P.-J.; Yagiz, K.; Balicki, A.; Kim, C.; Morré, D. M. ECTO-NOX target for the anticancer isoflavone phenoxodiol. Oncol. Res. 16:299–312; 2007.
7. Kurkjian, C.; Pat, S.; Burris, H. A.; Bendell, J. C.; Jones, S. F.; Moore, K. N.; Moreno, O.; Mass, R. D.; Infante, J. R. ME-143, a novel inhibitor of tumor-specific NADH oxidase (tNOX). Results from a first-in-human phase I study. J. Clin. Oncol. 30(Suppl. abstr. 3067); 2012.
8. Kelly, G. Interim results of a phase Ib/IIa study of oral phenoxodiol in patients with late-stage, hormone-refractory prostate cancer. Proc. Am. Assoc. Cancer Res. 45(Suppl. 1): 103–104; 2004.
9. Wilkinson, E. Phenoxodiol offers hope for ovarian cancer. Lancet Oncol. 5:201; 2004.
10. Goss, G.; Quinn, M.; Rutherford, T.; Kelly, G. A randomized Phase II study of phenoxodiol with platinum or taxane chemotherapy in chemoresistant epithelial ovarian cancer, fallopian tube cancer and primary peritoneal cancer. Eur. J. Cancer Suppl. 3:261; 2005.
11. Morré, D. J.; Morré, D. M. Cell surface NADH oxidases (ECTO-NOX proteins) with roles in cancer, cellular time--keeping, growth, aging and neurodegenerative diseases. Free Radic. Res. 37:795–808; 2003.
12. Morré, D. J. NADH oxidase: A multifunctional ectoprotein of the eukaryotic cell surface. In: Plasma membrane redox systems and their role in biological stress and disease. Dordrecht, The Netherlands: Kluwer Academic Publishers; 1998:121–156.
13. Chueh, P.-J.; Kim, C.; Cho, N.; Morré, D. M.; Morré, D. J. Molecular cloning and characterization of a tumor-associated, growth-related and time-keeping hydroquinone (NADH) oxidase (NOX) of the HeLa cell surface. Biochemistry 41:3732–3741; 2002.
14. Morré, D. J.; Reust, T. A. Circulating form of NADH oxidase activity responsive to the antitumor sulfonylurea N-(4-methylphenylsulfonyl)-N'-(4-chlorophenyl)urea (LY18 1984) specific to sera of cancer patients. J. Bioenerg. Biomembr. 29:281–289; 1997.
15. Morré, D. J.; Caldwell, S.; Mayorga, A.; Wu, L.-Y.; Morré, D. M. NADH oxidase activity from sera altered by capsaicin is widely distributed among cancer patients. Arch. Biochem. Biophys. 342:224–230; 1997.
16. Morré, D. J.; Chueh, P.-J.; Morré, D. M. Capsaicin inhibits preferentially the NADH oxidase and growth of transformed cells in culture. Proc. Natl. Acad. Sci. USA 91:1831–1835; 1995.
17. Alonso, M. M.; Encio, I.; Martinez-Merion, V.; Gil, M.; Migliaccio, M. New cytotoxic benzo(b)thiophenilsulfonamide 1,1-dioxide derivatives inhibit a NADH oxidase located in plasma membranes of tumour cells. Br. J. Cancer 85:1400–1402; 2001.
18. Chueh, P.-J.; Wu, L.-Y.; Morré, D. M.; Morré, D. J. tNOX is both necessary and sufficient as a cellular target for the anticancer actions of capsaicin and the green tea catechin (-)-epigallocatechin-3-gallate. BioFactors 20:249–263; 2004.
19. Morré, D. J.; Bridge, A.; Wu, L.-Y.; Morré, D. M. Preferential inhibition by (–)- epigallocatechin-3-gallate of the cell surface NADH oxidase and growth of transformed cells in culture. Biochem. Pharmacol. 60:937–946; 2000.
20. Morré, D. J.; Morré, D. M; Stevenson, J.; MacKellar, W.; McClure, D. HeLa plasma membranes bind the antitumor sulfonylurea LY181984 with high affinity. Biochim. Biophys. Acta 1244:133–140; 1995.
21. Kaplan, N. O. The pyridine coenzymes. In: The enzymes (vol. 3), Boyer, P. D.; Lardy, H.; Myrbäck, K., eds. New York: Academic Press;1959:105–169.
22. Morré, D. J.; Morré, D. M. Spectroscopic analyses of oscillations in ECTO-NOX catalyzed oxidation of NADH. Nonlinearity Biol. Toxicol. Med. 1:345–362; 2003.
23. Morré, D. J.; Gomez-Rey, M. L.; Schramke, C.; Em, O.; Lawler, J.; Hobeck, J.; Morré, D. M. Use of dipyridyl-dithio substrates to measure directly the protein disulfide-thiol interchange activity of the auxin stimulated NADH: Protein disulfide reductase of soybean plasma membranes. Mol. Cell. Biochem. 200:7–13; 1999.
24. Kishi, T.; Morré, D. M.; Morré, D. J. The plasma membrane NADH oxidase of HeLa cells has hydroquinone oxidase activity. Biochim. Biophys. Acta 1412:66–77; 1999.
25. Hatefi, Y. Coenzyme Q (ubiquinone). Adv. Enzymol. Relat. Areas Mol. Biol. 25:275–328; 1963.
26. Sun, I. L.; Sun, E. E.; Crane, F. L.; Morré, D. J.; Lindgren, A.; Low, H. Requirement for coenzyme Q in plasma membrane electron transport. Proc. Natl. Acad. Sci. USA 89: 11126–11130; 1992.
27. Smith, P. K.; Krohn, R. I.; Hermanson, G. T; Mailia, A K.; Gartner, F. H.; Provenzano, M. D.; Fujimoto, E. K.; Goeke, N. M.; Olson, B. J.; Klenk, D. C. Measurement of protein using bicinchoninic acid. Anal. Biochem. 150:76–85; 1985.
28. Foster, K.; Anwar, N.; Pogue, R.; Morré, D. M.; Keenan, T. W.; Morré, D. J. Decomposition analyses applied to a complex ultradian biorhythm: The oscillating NADH oxidase activity of plasma membranes having a potential time-keeping (clock) function. Nonlinearity Biol. Toxicol. Med. 1:51–70; 2003.
29. Tang, X; Morré, D. J.; Morré, D. M. Antisense experiments demonstrate an exon 4 minus splice variant mRNA as the basis for expression of tNOX, a cancer-specific cell surface protein. Oncol. Res. 16:557–567; 2008.
30. del Castillo-Olivares, A.; Yantiri, F.; Chueh, P.-J.; Wang, S.; Sweeting, M.; Sedlak, D.; Morré, D. M.; Burgess, J.; Morré, D. J. A drug-responsive and protease-resistant 34 kD NADH oxidase from the surface of HeLa cells. Arch. Biochem. Biophys. 358:125–140; 1998.
31. Morré, D. J.; Chueh, P.-J.; Lawler, J.; Morré, D. M. The sulfonylurea-inhibited NADH oxidase activity of HeLa cell plasma membranes has properties of a protein disulfide-thiol oxidoreductase with protein disulfide-thiol interchange activity. J. Bioenerg. Biomemb. 30:477–487; 1998.
32. Morré, D. J.; Kim, C.; Paulik, M.; Morré, D. M.; Faulk, W. P. Is the drug-responsive NADH oxidase of the cancer cell plasma membrane a molecular target for adriamycin? J. Biomemb. Bioenerg. 29:269–280; 1997.

33. Morré, D. J. NADH oxidase activity of HeLa plasma membranes inhibited by the antitumor sulfonylurea N-(4-methylphenylsulfonyl)-N'-(4-chlorophenyl)urea (LY181984) at an external site. Biochim. Biophys. Acta 1240:201–208; 1995.
34. Morré, D. J.; Wu, L.-Y.; Morré, D. M. The antitumor sulfonylurea N-(4- methylphenylsulfonyl)-N'-(chlorophenyl)urea (LY181984) inhibits NADH oxidase activity of HeLa plasma membrane. Biochim. Biophys. Acta 1240:11–17; 1995.
35. Wang, S.; Pogue, R.; Morré, D. M.; Morré, D. J. NADH oxidase activity (NOX) and enlargement of HeLa cells oscillate with two different temperature-compensated period lengths of 22 and 24 minutes corresponding to different NOX forms. Biochim. Biophys. Acta 1539:192–204; 2001.
36. Morgan, D. O. Cyclin-dependent kinases: Engines, clocks, and microprocessors. Ann. Rev. Cell Dev. Biol. 13:261–291; 1997.
37. Morré, D. J.; Chueh, P.-J.; Pletcher, J.; Tang, X.; Wu, L.-Y.; Morré, D. M. Biochemical basis for the biological clock. Biochemistry 40:11941–11945; 2002.
38. Morré, D. J; Lawler, J.; Wang, S.; Keenan, T. W.; Morré, D. M. Entrainment in solution of an oscillating NADH oxidase activity from the bovine milk fat globule membrane with a temperature-compensated period length suggestive of an ultradian time-keeping (clock) function. Biochim. Biophys. Acta 1559:10–20; 2002.
39. Morré, D. J.; Morré, D. M. The plasma membrane-associated NADH oxidase(ECTONOX) of mouse skin responds to blue light. J. Photochem. Photobiol. B 70:7–12; 2003.
40. Edmunds, L. N. Cellular and molecular basis of biological clocks. New York, Berlin, Heidelberg: Springer-Verlag; 1988.
41. Dunlap, J. C. Genetics and molecular analysis of circadian rhythms. Annu. Rev. Genetics 30:576–601; 1996.
42. Panka, D. J.; Mano, T.; Suhara, T.; Walsh, K.; Mier, J. W. Phosphatidylinositol 3- kinase/Akt activity regulates c-FLIP expression in tumor cells. J. Biol. Chem. 276:6893–6896; 2001.
43. Suhara, T.; Mano, T.; Oliveira, B. E.; Walsh, K. Phosphatidylinositol 3-kinase/Akt signaling controls endothelial cell sensitivity to Fas-mediated apoptosis via regulation of FLICE-inhibitory protein (FLIP). Circ. Res. 89:13–19; 2001.
44. DeLuca, T.; Morré, D. M.; Zhao, H.; Morré, D. J. NAD+ /NADH and/or CoQ/CoQH2 ratios from plasma membrane electron transport may determine ceramide and sphingosine-1-phosphate levels accompanying G1 arrest and apoptosis. BioFactors 25:43–60; 2006.
45. De Luca, T.; Morré, D. J.; Morré, D. M. Reciprocal relationship between cytosolic NADH and ENOX2 inhibition triggers sphingolipid-induced apoptosis in HeLa cells. J. Cell. Biochem. 110:1504–1511; 2010.
46. Morré, D. J.; Morré, D. M. Synergistic capsicum-tea mixtures with anticancer activity. J. Pharm. Pharmacol. 55: 987–994; 2003.
47. Morré, D. J.; Merriman, R.; Tanzer, L. R.; Wu, L.-Y.; Morré, D. M.; MacKellar, W. C. Inhibition of the NADH oxidase activity of plasma membranes isolated from xenografts and cell lines by the antitumor sulfonylurea, N-(4-methylphenylsulfonyl)-N(4-chlorophenyl)urea (LY181984) correlates with drug susceptibility of growth. Protoplasma 184:203–208; 1994.
48. Morré, D. J.; Morré, D. M. ECTO-NOX Proteins. Springer, New York, 507 pp. 2013.
49. Morré, D. J.; Dick, S.; Bosneaga, E.; Balicki, A.; Wu, L.-Y.; McClain, W.; Morré, D. M. tNOX (ENOX1) target for chemosensitization-low-dose responses in the hermetic concentration range. Am. J. Pharmacol. Toxicol. 3:16–26; 2008.
50. Morré, D. J.; McClain, N.; Wu, L.-Y.; Kelly, G.; Morré, D. M. Phenoxodiol treatment alters the subsequent response of tNOX and growth of HeLa cells to paclitaxel and cisplatin. Mol. Biotechnol. 42:100–109; 2009.